Two-point probability function for distributions of oriented hard ellipsoids

F. Lado
Department of Physics, North Carolina State University, Raleigh, North Carolina 27695-8202
S. Torquato
Department of Mechanical and Aerospace Engineering and Department of Chemical Engineering, North Carolina State University, Raleigh, North Carolina 27695-7910

(Received 30 April 1990; accepted 2 July 1990)

The macroscopic properties of two-phase random heterogeneous media depend upon an infinite sequence of n-point functions $S_n^{(i)}(\mathbf{x}_1,\mathbf{x}_2,...,\mathbf{x}_n)$ giving the joint probability of finding n points with positions $\mathbf{x}_1,\mathbf{x}_2,...,\mathbf{x}_n$ all in phase i. This paper reports the first study and calculation of the two-point probability function $S_2^{(i)}$ for distributions of oriented, hard spheroids with eccentricity ϵ in a matrix. This is a useful model of statistically anisotropic two-phase media, enabling one to examine the special limiting cases of oriented disks ($\epsilon = 0$), spheres ($\epsilon = 1$), and oriented needles ($\epsilon = \infty$).

I. INTRODUCTION

Two-phase heterogeneous materials abound in nature and in manmade situations. Examples of such media include fluid-saturated sandstones, slurries, blood, animal and plant tissue, fiber-epoxy composites, particulate composites, freeze-dried foods, microemulsions, cermets, and soils. It is known that the macroscopic properties of such materials (e.g., transport, mechanical, optical, and electromagnetic properties) depend upon the details of the microstructure.[1-7] The microstructure can be completely characterized by specifying any of the various infinite sets of statistical correlation functions that have been defined in the past.[8] One such correlation function is the so-called n-point probability function $S_n^{(i)}(\mathbf{x}_1,\mathbf{x}_2,...,\mathbf{x}_n)$, which gives the joint probability of finding n points with positions $\mathbf{x}_1,\mathbf{x}_2,...,\mathbf{x}_n$ all in phase i. This function has been shown to arise in rigorous expressions for the effective conductivity of composites,[1-4] fluid permeability of porous media,[5-6] trapping constant associated with diffusion-controlled processes among static traps,[7] and the elastic moduli of composites.[9]

In the last decade considerable progress has been made in representing and computing the $S_n^{(i)}$ for *isotropic* models consisting of distributions of spheres in a matrix.[10-12] Although the extension of this formalism to represent the $S_n^{(i)}$ for statistically *anisotropic* distributions of particles is formally straightforward,[4] calculation of the resulting series representations of the n-point functions is substantially more difficult for such media. Indeed, the two-point probability function $S_2^{(i)}$ has only recently been computed for overlapping, oriented cylinders of finite aspect ratio in order to bound the effective conductivity tensor of such a model.[4] Therefore, evaluation of effective properties of statistically anisotropic two-phase media (e.g., aligned, short-fiber composites), an important class of materials, has been very limited and has received little attention. The purpose of this paper is to study and calculate the two-point probability function $S_2^{(i)}$ for a distribution of oriented spheroids with eccentricity ϵ in a matrix. Interesting limiting cases of such a model are oriented disks ($\epsilon = 0$), spheres ($\epsilon = 1$), and oriented needles ($\epsilon = \infty$).

II. TWO-POINT PROBABILITY FUNCTION FOR ORIENTED ELLIPSOIDS

We consider a statistically homogeneous system of oriented (i.e., aligned) hard ellipsoids embedded in a matrix. In the parlance of two-phase random media, the matrix constitutes phase 1, whose domain is D_1 in the total volume V and occupies volume fraction ϕ_1, while the included ellipsoids make up phase 2, having the complementary domain D_2 and volume fraction $\phi_2 = 1 - \phi_1$. The effective properties of such composites are completely characterized by an infinite sequence of n-point functions $S_n^{(i)}(\mathbf{x}_1,\mathbf{x}_2,...,\mathbf{x}_n)$ giving the joint probability of finding n points with positions $(\mathbf{x}_1,\mathbf{x}_2,...,\mathbf{x}_n) \equiv \mathbf{x}^n$ all in phase i. The formal study of these n-point probability functions was initiated by Torquato and Stell[10] for isotropic media; explicit extensions of the formalism to anisotropic media have been considered by Torquato and Sen.[4] Here we need only recall some basic definitions from these works for completeness while specializing them to the case of oriented spheroids.

Let $I^{(i)}(\mathbf{x})$ be a random variable of position $\mathbf{x}$ characterizing phase i,

$$I^{(i)}(\mathbf{x}) = \begin{cases} 1, & \mathbf{x} \in D_i, \\ 0, & \text{otherwise.} \end{cases} \tag{1}$$

The general n-point probability function for phase i is then defined by

$$S_n^{(i)}(\mathbf{x}^n) = \left\langle \prod_{j=1}^{n} I^{(i)}(\mathbf{x}_j) \right\rangle, \tag{2}$$

where the angular brackets denote an equilibrium average over all configurations of the inclusions. For "hard" inclusions, this is simply an average over all configurations having no overlaps of the included shapes.

Equation (2) can be made more explicit by introducing a spheroid indicator function $m(\mathbf{r})$. Let the axially symmetric spheroids be aligned with their symmetry axis in the z-direction. Then with $\mathbf{r}$ measured from the center of mass of a spheroid, the function

 0021-9606/90/205912-06$03.00

$$m(\mathbf{r}) = \begin{cases} 1, & \dfrac{x^2+y^2}{a^2} + \dfrac{z^2}{b^2} < 1, \\ 0, & \text{otherwise} \end{cases} \tag{3}$$

characterizes the interior of the spheroid with semiaxes a and b. The matrix characteristic function for N such inclusions in the volume V is then expressible as

$$I^{(1)}(\mathbf{x}) = \prod_{i=1}^{N} [1 - m(\mathbf{x} - \mathbf{r}_i)], \tag{4}$$

where $\mathbf{r}_i$ locates the center of mass of spheroid i. Now put

$$M(\mathbf{r}_i;\mathbf{x}^n) \equiv 1 - \prod_{j=1}^{n} [1 - m(\mathbf{x}_j - \mathbf{r}_i)] = \begin{cases} 0, & \text{if } \textit{none} \text{ of the } \mathbf{x}_j \text{ lie in spheroid } i, \\ 1, & \text{otherwise.} \end{cases} \tag{5}$$

It follows then with (4) and (5) that

$$\prod_{j=1}^{n} I^{(1)}(\mathbf{x}_j) = \prod_{i=1}^{N} \prod_{j=1}^{n} [1 - m(\mathbf{x}_j - \mathbf{r}_i)] = \prod_{i=1}^{N} [1 - M(\mathbf{r}_i;\mathbf{x}^n)]$$
$$= 1 - \sum_{i=1}^{N} M(\mathbf{r}_i;\mathbf{x}^n) + \sum_{i<j} M(\mathbf{r}_i;\mathbf{x}^n) M(\mathbf{r}_j;\mathbf{x}^n) - \sum_{i<j<k} M(\mathbf{r}_i;\mathbf{x}^n) M(\mathbf{r}_j;\mathbf{x}^n) M(\mathbf{r}_k;\mathbf{x}^n) + \cdots . \tag{6}$$

If the conclusions cannot overlap each other, this series terminates when there are more inclusions $\mathbf{r}_i$ than points $\mathbf{x}_j$.[11] That is, for products of more than n of the $M(\mathbf{r}_i;\mathbf{x}^n)$ at least one of the ellipsoids will necessarily be devoid of any $\mathbf{x}_j$ and by Eq. (5) the product vanishes for all allowed configurations. Putting the truncated expansion (6) into Eq. (2) and making use of the interchangeability of particle labels $\mathbf{r}_i$ in the averaging integral then yields

$$S_n^{(1)}(\mathbf{x}^n) = 1 + \sum_{k=1}^{n} (-1)^k \frac{N!}{k!(N-k)!} \left\langle \prod_{j=1}^{k} M(\mathbf{r}_j;\mathbf{x}^n) \right\rangle$$
$$= 1 + \sum_{k=1}^{n} \frac{(-1)^k}{k!} \int \rho_k(\mathbf{r}^k) \prod_{j=1}^{k} [M(\mathbf{r}_j;\mathbf{x}^n) d\mathbf{r}_j], \tag{7}$$

where we have introduced the k-particle density function[13] for the inclusions,

$$\rho_k(\mathbf{r}_1',\mathbf{r}_2',\ldots,\mathbf{r}_k') = \frac{N!}{(N-k)!} \left\langle \prod_{j=1}^{k} \delta(\mathbf{r}_j' - \mathbf{r}_j) \right\rangle. \tag{8}$$

For a statistically homogeneous system, even if not isotropic, the origin of coordinates is arbitrary and these distributions become functions of relative coordinates,

$$\rho_k(\mathbf{r}_1,\mathbf{r}_2,\ldots,\mathbf{r}_k) = \rho_k(\mathbf{r}_{12},\ldots,\mathbf{r}_{1k}) = \rho^k g_k(\mathbf{r}_{12},\ldots,\mathbf{r}_{1k}). \tag{9}$$

The second equality of (9) defines the dimensionless k-particle distribution function g_k, where we have used $\rho = \rho_1(\mathbf{r}_1) = N/V$.

In this work we are primarily interested in $S_2^{(1)}(\mathbf{x}_{12})$, which depends on $g_2(\mathbf{r}_{12})$ for aligned ellipsoids. The calculation of the anisotropic $g_2(\mathbf{r}_{12})$ is described below. Here we note in passing that, from (7) and (9),

$$S_1^{(1)}(\mathbf{x}_1) = 1 - \rho \int M(\mathbf{r}_1;\mathbf{x}_1) d\mathbf{r}_1 = 1 - \rho \int m(\mathbf{r}) d\mathbf{r} = 1 - \rho V_1 = 1 - \phi_2 = \phi_1, \tag{10}$$

as expected, where $V_1 = \frac{4}{3}\pi a^2 b$ is the volume of an ellipsoid.

The two-point matrix probability function can be somewhat simplified as follows. We have

$$S_2^{(1)}(\mathbf{x}_{12}) = 1 - \rho \int M(\mathbf{r}_1;\mathbf{x}_1,\mathbf{x}_2) d\mathbf{r}_1 + \frac{1}{2}\rho^2 \int g_2(\mathbf{r}_{12}) M(\mathbf{r}_1;\mathbf{x}_1,\mathbf{x}_2) \times M(\mathbf{r}_2;\mathbf{x}_1,\mathbf{x}_2) d\mathbf{r}_1 \, d\mathbf{r}_2$$
$$= 1 - \rho V_2(\mathbf{x}_{12}) + \rho^2 U_2(\mathbf{x}_{12}). \tag{11}$$

Here, $V_2(\mathbf{x}_{12})$ is the union volume of two aligned spheroids whose centers of mass are separated by $\mathbf{x}_{12}$,

$$V_2(\mathbf{x}_{12}) = \int M(\mathbf{r}_1;\mathbf{x}_1,\mathbf{x}_2) d\mathbf{r}_1 = \int [m(\mathbf{x}_1 - \mathbf{r}_1) + m(\mathbf{x}_2 - \mathbf{r}_1) - m(\mathbf{x}_1 - \mathbf{r}_1) m(\mathbf{x}_2 - \mathbf{r}_1)] d\mathbf{r}_1$$
$$= 2V_1 - V_2^*(\mathbf{x}_{12}), \tag{12}$$

where $V_2^*(\mathbf{x}_{12})$ is then the corresponding intersection volume. Similarly, for $U_2(\mathbf{x}_{12})$ we write first

$$U_2(\mathbf{x}_{12}) = \frac{1}{2} \int g_2(\mathbf{r}_{12}) [m(\mathbf{x}_1 - \mathbf{r}_1) + m(\mathbf{x}_2 - \mathbf{r}_1) - m(\mathbf{x}_1 - \mathbf{r}_1) m(\mathbf{x}_2 - \mathbf{r}_1)] \times [m(\mathbf{x}_1 - \mathbf{r}_2) + m(\mathbf{x}_2 - \mathbf{r}_2) - m(\mathbf{x}_1 - \mathbf{r}_2) m(\mathbf{x}_2 - \mathbf{r}_2)] d\mathbf{r}_1 \, d\mathbf{r}_2$$
$$= \int g_2(\mathbf{r}_{12}) m(\mathbf{x}_1 - \mathbf{r}_1) m(\mathbf{x}_2 - \mathbf{r}_2) d\mathbf{r}_1 \, d\mathbf{r}_2, \tag{13}$$

where other terms in (13) vanish since, without overlap of the two spheroids, any given $\mathbf{x}_i$ cannot be in both. Next, we introduce the total correlation function $h(\mathbf{r}_{12}) = g_2(\mathbf{r}_{12}) - 1$ to write

$$U_2(\mathbf{x}_{12}) = \left[\int m(\mathbf{r})d\mathbf{r}\right]^2 + \int h(\mathbf{r}_{12})m(\mathbf{x}_1 - \mathbf{r}_1) \times m(\mathbf{x}_2 - \mathbf{r}_2)d\mathbf{r}_1\, d\mathbf{r}_2 = V_1^2 + U_2^*(\mathbf{x}_{12}). \quad (14)$$

Thus, $S_2^{(1)}(\mathbf{x}_{12})$ in (11) becomes

$$S_2^{(1)}(\mathbf{x}_{12}) = 1 - 2\rho V_1 + \rho^2 V_1^2 + \rho V_2^*(\mathbf{x}_{12}) + \rho^2 U_2^*(\mathbf{x}_{12}), = \phi_1^2 + S_2^*(\mathbf{x}_{12}), \quad (15)$$

with

$$S_2^*(\mathbf{x}_{12}) = S_2^{(1)}(\mathbf{x}_{12}) - \phi_1^2 = \rho V_2^*(\mathbf{x}_{12}) + \rho^2 U_2^*(\mathbf{x}_{12}). \quad (16)$$

For widely separated points $\mathbf{x}_1$ and $\mathbf{x}_2$, $S_2^{(1)}(\mathbf{x}_{12})$ becomes simply ϕ_1^2, so that its subtraction in (16) yields a function $S_2^*(\mathbf{x}_{12})$ that vanishes for large argument; further, it is the same function for both phases, so that no superscript need be written. Thus the task at hand is to evaluate

$$V_2^*(\mathbf{x}_{12}) = \int m(\mathbf{x}_1 - \mathbf{r}_1)m(\mathbf{x}_2 - \mathbf{r}_1)d\mathbf{r}_1 \quad (17a)$$

and

$$U_2^*(\mathbf{x}_{12}) = \int h(\mathbf{r}_{12})m(\mathbf{x}_1 - \mathbf{r}_1)m(\mathbf{x}_2 - \mathbf{r}_2)d\mathbf{r}_1\, d\mathbf{r}_2 \quad (17b)$$

for aligned spheroids.

What makes this task reasonably straightforward is the observation by Lebowitz and Perram[14] that a scale transformation to coordinates

$$\mathbf{R} \equiv (X,Y,Z) = \left(x,y,\frac{a}{b}z\right) \quad (18)$$

converts the spheroids of shape

$$\frac{x^2+y^2}{a^2} + \frac{z^2}{b^2} = 1 \quad (19)$$

into spheres of radius a, thus reducing the thermodynamics and particle correlations of aligned hard spheroids to an equivalent problem involving hard spheres, a much-studied model in the theory of liquids.[13] From (18) we extract the radial coordinate R as

$$R^2 = x^2 + y^2 + \frac{a^2}{b^2}z^2 = r^2 + \left(\frac{a^2}{b^2} - 1\right)z^2, \quad (20)$$

or

$$R = r[1 - (1 - a^2/b^2)\cos^2\theta\,]^{1/2} = 2ar/\sigma(\theta), \quad (21)$$

where θ is the polar angle between the z axis and $\mathbf{r} = (x,y,z)$. In (21) we have defined an angle-dependent "hard sphere diameter"

$$\sigma(\theta) = \frac{2a}{[1 - (1 - a^2/b^2)\cos^2\theta\,]^{1/2}}. \quad (22)$$

With this insight, we can proceed immediately to the calculation of the intersection volume V_2^*. For two hard spheres of radius a separated by a center-to-center distance R_{12}, this quantity is

$$V_{2(\mathrm{HS})}^*(R_{12}) = \int m_{\mathrm{HS}}(R_{13})m_{\mathrm{HS}}(R_{32})d\mathbf{R}_3 = \frac{4}{3}\pi a^3\left[1 - \frac{3}{2}\left(\frac{R_{12}}{\sigma_o}\right) + \frac{1}{2}\left(\frac{R_{12}}{\sigma_o}\right)^3\right] \times H(\sigma_o - R_{12}), \quad (23)$$

where $\sigma_o \equiv 2a$ is the sphere diameter,

$$m_{\mathrm{HS}}(R) = \begin{cases} 1, & R < a, \\ 0, & R > a, \end{cases} \quad (24)$$

and $H(x)$ is the Heaviside unit function,

$$H(x) = \begin{cases} 1, & x > 0, \\ 0, & x < 0. \end{cases} \quad (25)$$

For oriented hard ellipsoids, the coordinate transformation (18) yields

$$V_2^*(\mathbf{r}_{12}) = \int m(\mathbf{r}_{13})m(\mathbf{r}_{32})d\mathbf{r}_3 = \frac{b}{a}\int m_{\mathrm{HS}}(R_{13})m_{\mathrm{HS}}(R_{32})dR_3 = \frac{4}{3}\pi a^2 b\left[1 - \frac{3}{2}\left(\frac{r_{12}}{\sigma(\theta)}\right) + \frac{1}{2}\left(\frac{r_{12}}{\sigma(\theta)}\right)^3\right] \times H(\sigma(\theta) - r_{12}), \quad (26)$$

where we have used (23) and (21). More briefly, Eq. (26) can be written

$$V_2^*(\mathbf{r}_{12}) = \frac{b}{a}V_{2(\mathrm{HS})}^*\left(\sigma_o\frac{r_{12}}{\sigma(\theta)}\right). \quad (27)$$

This completes the evaluation of (17a).

For (17b), a closed form expression such as Eq. (26) cannot be given since none exists for hard spheres. However, a simple scaled relationship like Eq. (27) is immediate;

$$U_2^*(\mathbf{r}_{12}) = \int h(\mathbf{r}_{34})m(\mathbf{r}_{13})m(\mathbf{r}_{42})d\mathbf{r}_3\, d\mathbf{r}_4 = (b/a)^2\int h_{\mathrm{HS}}(R_{34})m_{\mathrm{HS}}(R_{13})m_{\mathrm{HS}}(R_{42}) \times d\mathbf{R}_3\, d\mathbf{R}_4 = (b/a)^2 U_{2(\mathrm{HS})}^*(R_{12}) = (b/a)^2 U_{2(\mathrm{HS})}^*(\sigma_o r_{12}/\sigma(\theta)). \quad (28)$$

Thus, we need but compute $U_{2(\mathrm{HS})}^*(R)$ to obtain $U_2^*(\mathbf{r})$ by interpolation.

Since Eq. (28) involves a double convolution, the calculation of $U_{2(\mathrm{HS})}^*(R)$ is most easily carried out using Fourier transforms. For the hard-sphere version of (28) we then have in transform space

$$\tilde{U}^*_{2(\mathrm{HS})}(k) = \tilde{h}_{\mathrm{HS}}(k)\tilde{m}^2_{\mathrm{HS}}(k). \tag{29}$$

For radially symmetric functions $f(r)$ the three-dimensional Fourier transform reduces to

$$\tilde{f}(k) = \frac{4\pi}{k}\int_0^\infty dr\, r f(r)\sin kr, \tag{30a}$$

with the inverse

$$f(r) = \frac{1}{2\pi^2 r}\int_0^\infty dk\, k\tilde{f}(k)\sin kr. \tag{30b}$$

Evaluating (30a) for $m_{\mathrm{HS}}(r)$ gives

$$\tilde{m}_{\mathrm{HS}}(k) = \frac{4\pi}{k^3}(\sin ka - ka\cos ka). \tag{31}$$

The final quantity needed is $\tilde{h}_{\mathrm{HS}}(k)$. No exact expression for the hard sphere pair correlation function $h_{\mathrm{HS}}(r)$ is known. However, an excellent approximation is available from the solution of the Percus–Yevick (PY) integral equation for a hard sphere fluid. In PY approximation, the related direct correlation function $C_{\mathrm{HS}}(r)$ is given by[13]

$$C_{\mathrm{HS}}(r) = A_1 + A_2\left(\frac{r}{\sigma_o}\right) + A_3\left(\frac{r}{\sigma_o}\right)^3, \quad r<\sigma_o$$
$$= 0, \quad r>\sigma_o. \tag{32}$$

Here, the coefficients are

$$A_1 = -(1+2\eta)/(1-\eta)^4,$$
$$A_2 = 6\eta(1+\eta/2)/(1-\eta)^4,$$
$$A_3 = \eta A_1/2, \tag{33}$$

where

$$\eta = \frac{4}{3}\pi\rho_{\mathrm{HS}}a^3 \tag{34}$$

is the volume fraction of the hard spheres, which is *set equal* to ϕ_2 for the ellipsoids; i.e., $\rho_{\mathrm{HS}} = (b/a)\rho$. The connection between $h_{\mathrm{HS}}(r)$ and $C_{\mathrm{HS}}(r)$ is through the Ornstein–Zernike equation,[14] which in Fourier transform space reads

$$\tilde{h}_{\mathrm{HS}}(k) = \frac{\tilde{C}_{\mathrm{HS}}(k)}{1-\rho_{\mathrm{HS}}\tilde{C}_{\mathrm{HS}}(k)}. \tag{35}$$

The transform of $C_{\mathrm{HS}}(r)$ can be readily obtained analytically from Eq. (32), but we omit the result because of length.

This completes the steps needed to determine $U^*_{2(\mathrm{HS})}(R_{12})$: combine Eqs. (31) and (35) in Eq. (29) and invert with Eq. (30b). The Fourier inversion must be done numerically. With $U^*_{2(\mathrm{HS})}(R_{12})$ in hand, the desired anisotropic $U^*_2(\mathbf{r}_{12})$ is obtained by interpolation using Eq. (28).

The PY approximation for $\tilde{h}_{\mathrm{HS}}(k)$ is the sole approximation used in computing $S^*_2(\mathbf{r}_{12})$.

III. RESULTS FOR $S^*_2(\mathbf{r}_{12})$ OF ORIENTED HARD ELLIPSOIDS

We have computed $S^*_2(\mathbf{r}) = S^*_2(r,\theta)$ for a variety of ellipsoid volume fractions ϕ_2 and eccentricities $\epsilon = b/a$. As noted below, the oblate ($\epsilon<1$) results are related to the prolate ($\epsilon>1$) by a simple symmetry, so that we have selected for display a sampling of $S^*_2(r,\theta)$ for prolate spheroids.

Figures 1 and 2 show cross sections of $S^*_2(r,\theta)$ for a low density system with $\phi_2 = 0.2$. In Fig. 2, we see the effects of anisotropy for $\epsilon = b/a = 2$ in the form of cross sections through $S^*_2(r,\theta)$ for $\theta = 0$, 45°, and 90°, reading from right to left on the main peak of the curves. Note that the distance is in units of the major semiaxis b, so that the curve for $\theta = 0$ (the outermost of the three) is identical to the hard sphere limit.[11] This remains true for the results shown in Fig. 2, corresponding to $\epsilon = 10$. With b as the unit of distance in both these cases, the $\theta = 0$ cross section remains unchanged while the others move progressively toward smaller r as ϵ increases, reflecting the increasing disparity of the inclusion asymmetry.

The same set of cross sections is shown in Figs. 3 and 4 for a high density situation, $\phi_2 = 0.6$. The basic shape of S^*_2 shows more pronounced structure over the low density cases in Figs. 1 and 2. As the eccentricity ϵ is increased from 2 to 10 in Figs. 3 and 4, respectively, the increased structure carries over to the cross-sections, taken again at $\theta = 0$, 45°, and 90°. Because the choice of distance scale is still the major semiaxis b, the $\theta = 0$ cross sections in these figures are again unchanged with respect to the spherical limit.[11] The contrast between the $\theta = 0$ cross section and that for $\theta = 90°$ for the needlelike case of $\epsilon = 10$ in Fig. 4 is particularly notable.

We remark that the value of S^*_2 at the origin is $\phi_1\phi_2$ in all cases.[10]

An alternative way to display the effects of anisotropy is to expand the two-point function $S^*_2(r,\theta)$ in Legendre polynomials $P_l(\cos\theta)$,

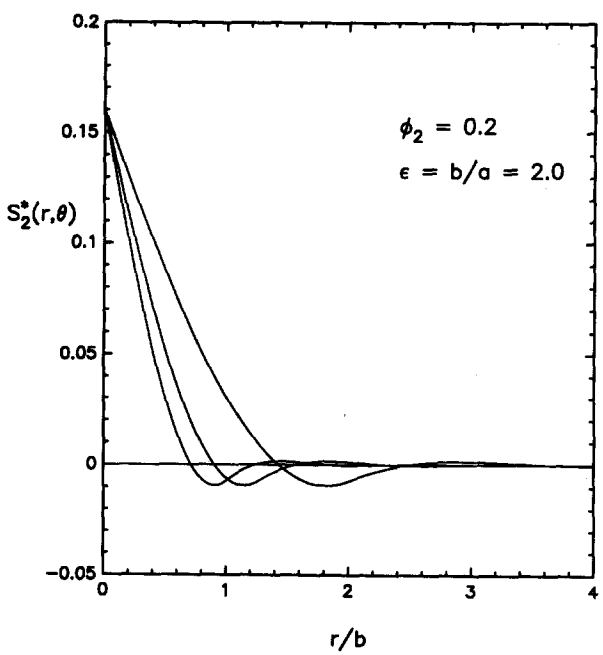

FIG. 1. Cross sections through the two-point probability function $S^*_2(r,\theta)$ for hard, oriented prolate spheroids at volume fraction $\phi_2 = 0.2$ and eccentricity $\epsilon = b/a = 2$. The curves are for $\theta = 0$, 45°, and 90°, read from right to left on the main peak.

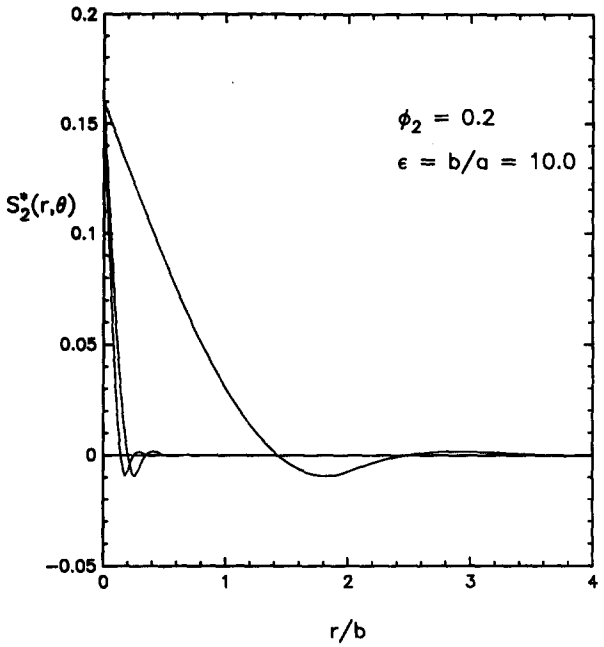

FIG. 2. Same as Fig. 1 with $\epsilon = 10$.

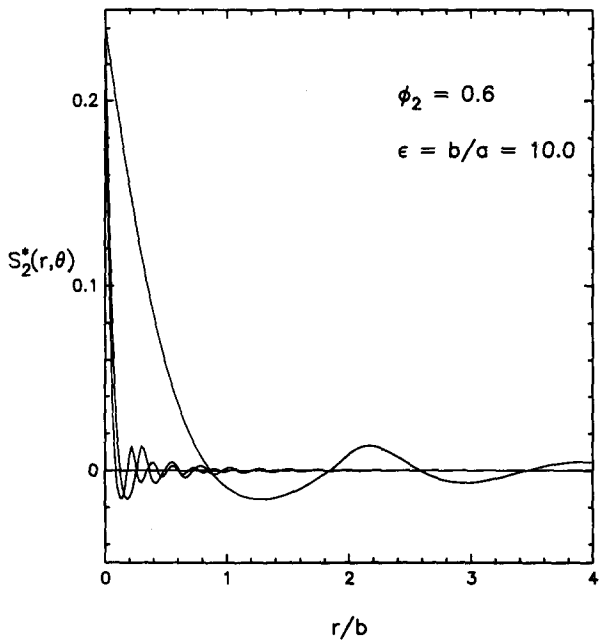

FIG. 4. Same as Fig. 3 for $\epsilon = 10$.

$$S_2^*(r,\theta) = \sum_{l=0}^{\infty} R_l(r) P_l(\cos\theta), \tag{36}$$

where

$$R_l(r) = (l + 1/2)\int_{-1}^{1} S_2^*(r,\theta) P_l(\cos\theta) d(\cos\theta). \tag{37}$$

Because of symmetry, only even values of l contribute to the expansion in (36).

Equation (37) was evaluated numerically using Gaussian quadrature. Figure 5 displays the radial coefficients $R_0(r)$, $R_2(r)$, $R_4(r)$, and $R_6(r)$ for $\epsilon = 2$ and $\phi_2 = 0.6$, which corresponds to the cross sections in Fig. 3. The coefficients are seen to progressively decrease in maximum amplitude and to pass through the first zero, to begin oscillations about zero at progressively larger ranges as l increases.

The effect of increasing anisotropy is seen in Fig. 6, which shows the same set of coefficients for $\epsilon = 10$ and unchanged volume fraction $\phi_2 = 0.6$ (cf. Fig. 4). Here the features of Fig. 5 are simply accentuated; it is apparent that the

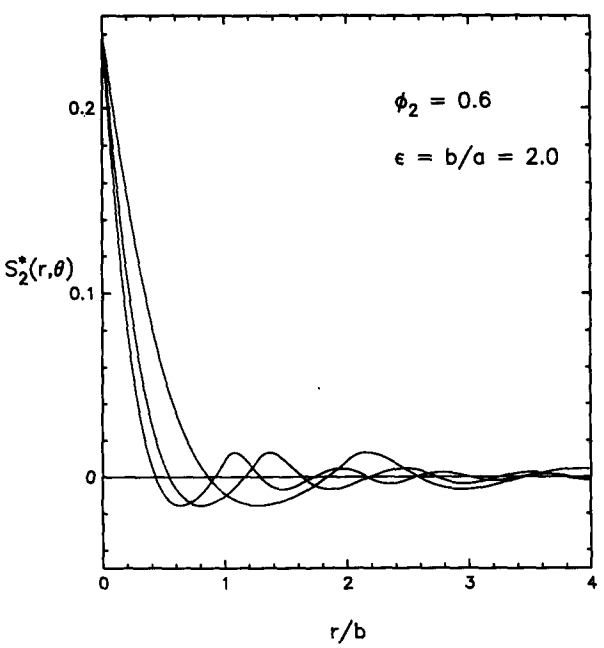

FIG. 3. Cross sections through the two-point probability function $S_2^*(r,\theta)$ for hard, oriented prolate spheroids at volume fraction $\phi_2 = 0.6$ and eccentricity $\epsilon = b/a = 2$. The curves for $\theta = 0, 45°$, and 90°, read from right to left on the main peak.

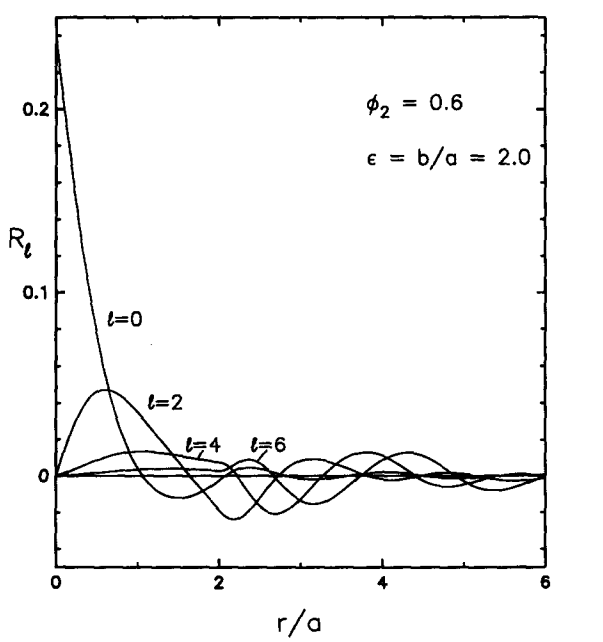

FIG. 5. Harmonic coefficients $R_l(r)$, $l = 0, 2, 4$, and 6, of $S_2^*(r,\theta)$ for hard, oriented prolate spheroids at volume fraction $\phi_2 = 0.6$ and eccentricity $\epsilon = b/a = 2$.

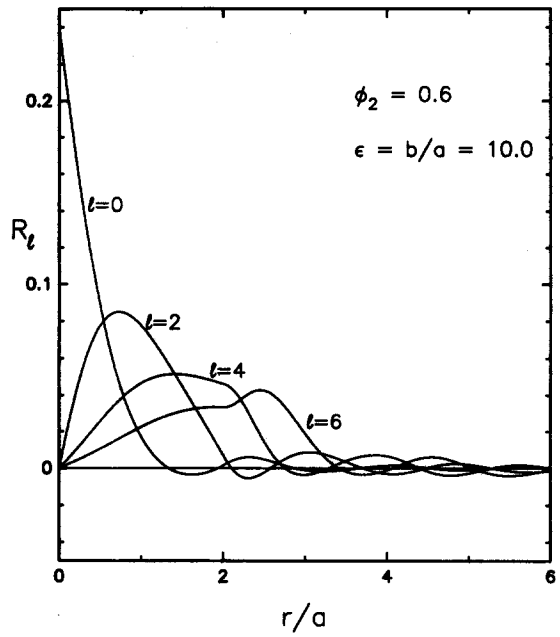

FIG. 6. Same as Fig. 5 for $\epsilon = 10$.

rate of convergence of the expansion (36) is much slower now than for the $\epsilon = 2$ case. Note that the scale of distance in Figs. 5 and 6 is the minor semiaxis a, which avoids a compression of the curves with increasing ϵ.

Cross sections of $S_2^*(r,\theta)$ for oblate spheroids, $\epsilon < 1$, can be computed in the same way. However, if the results are then plotted against r/a rather than r/b as in Figs. 1–4, they will be identical to the cross sections already displayed in these figures when the parameters are properly reinterpreted. This follows from the effective "hard sphere diameter" $\sigma(\theta)$ defined in Eq. (22), which is the key to the rescaled results of Eqs. (27) and (28). Writing $\sigma(\theta;\epsilon)$ to display the eccentricity parameter $\epsilon = b/a$ that is part of Eq. (22), we find easily from this equation that

$$\sigma(\theta;\epsilon)/b = \sigma(\pi/2 - \theta;1/\epsilon)/a. \tag{38}$$

This says in effect that the cross-sections for $\epsilon > 1$ in Figs. 1–4, plotted vs r/b, will be identical to cross sections for $\epsilon' = 1/\epsilon < 1$ when these are plotted vs r/a and read in reverse order for the angle θ. Thus, Figs. 1 and 3 and Figs. 2 and 4 translate immediately into equivalent results for $\epsilon = 0.5$ and $\epsilon = 0.1$, respectively, when interpreted in this fashion. This symmetry does not carry over to the radial coefficients shown in Figs. 5 and 6, which are qualitatively different for $\epsilon < 1$.

ACKNOWLEDGMENT

S. Torquato gratefully acknowledges the support of the Office of Basic Energy Sciences, U.S. Department of Energy, under Grant No. DEFG05-86ER13482.

[1] M. H. Beran, *Statistical Continuum Theories* (Wiley, New York, 1968).
[2] G. W. Milton, Phys. Rev. Lett. **46**, 542 (1981).
[3] S. Torquato, Rev. Chem. Eng. **4**, 151 (1987).
[4] S. Torquato and A. K. Sen, J. Appl. Phys. **67**, 1145 (1990).
[5] S. Prager, Phys. Fluids **4**, 1477 (1961); J. G. Berryman and G. W. Milton, J. Chem. Phys. **83**, 754 (1985).
[6] J. Rubinstein and S. Torquato, J. Fluid Mech. **206**, 25 (1989).
[7] J. Rubinstein and S. Torquato, J. Chem. Phys. **88**, 6372 (1988); S. Torquato and J. Rubinstein, *ibid.* **90**, 1644 (1989).
[8] S. Torquato, J. Stat. Phys. **45**, 843 (1986); Phys. Rev. B **35**, 5385 (1987).
[9] G. W. Milton and N. Phan-Thien, Proc. R. Soc. Lond. A **380**, 305 (1989).
[10] S. Torquato and G. Stell, J. Chem. Phys. **77**, 2071 (1982).
[11] S. Torquato and G. Stell, J. Chem. Phys. **82**, 980 (1985).
[12] See also the numerous references contained in Ref. 3.
[13] See, e.g., J. P. Hansen and I. R. McDonald, *Theory of Simple Liquids* (Academic, London, 1986).
[14] J. L. Lebowitz and J. W. Perram, Mol. Phys. **50**, 1207 (1983).